Supplementary Information

For

Unveiling a Potential Disinfection Process in Ultraviolet Treatment of Bromine-Containing Water: Inactivation of *P. aeruginosa* in UV/NH_2Br system

Shumin Zhu[ab], Jingxuan Yang[ab], Yangtao Wu[c], Da Sheng[ab *], Lingjun Bu[ab], Shiqing Zhou[ab]

a. Hunan Engineering Research Center of Water Security Technology and Application, College of Civil Engineering, Hunan University, Changsha 410082, PR China

b. Key Laboratory of Building Safety and Energy Efficiency, Ministry of Education, Hunan University, Changsha 410082, PR China

c. Department of Civil and Environmental Engineering, The Hong Kong Polytechnic University, Hung Hom, Kowloon, Hong Kong, China

** Corresponding author at: Key Laboratory of Building Safety and Energy Ef ciency, Ministry of Education, College of Civil Engineering, Hunan University, Changsha, Hunan, 410082, P.R. China.*

Email address: dsheng@hnu.edu.cn (Sheng. D)

Text S1. Chemicals.

Ultrapure water (18.2 MΩ·cm^{-1}) from the Milli-Q purification system (Millipore, Billerica, USA) is employed to prepare all stock solutions. sodium hydroxide ((NaOH, ≧96.0%), sulfuric acid (H_2SO_4, 95.0% ~ 98.0%), sodium chloride (analytical grade), sodium thiosulfate ($Na_2S_2O_3$, ≧99.0%), Sodium dihydrogen phosphate dihydrate ($Na_2HPO_4·2H_2O$, ≧99.0%), disodium hydrogen phosphate dodecahydrate ($NaH_2PO_4·12H_2O$, ≧99.0%), peptone (Beijing Aoboxing BIO-TECH CO.,LTD), beef extract powder (Qingdao Hope Bio-Technology Co. ,Ltd.), nutrient agar (Qingdao Hope Bio-Technology Co. ,Ltd.), ammonium chloride (NH_4Cl, ≧99.5%), propidium iodide (Thermo Fisher Scientific) and sodium hydrogen carbonate ($NaHCO_3$, ≧99.0%) were obtained from Aladdin (China). Reactive Oxygen Species Assay Kit was obtained from Beijing Solarbio Science & Technology Co., Ltd.

Text S2 Preparation of bacterial suspensions

The colonies from the activated plates were carefully scraped into Luria-Bertani (LB) broth and incubated with shaking at 37 ℃. The optical density at 600 nm (OD600) was monitored during the incubation process, and when it reached a value between 0.6 and 0.8, the bacterial cultures were subjected to centrifugation.

After centrifugation, the bacterial pellets were washed and resuspended using Phosphate buffer (PB). The concentration of *P. aeruginosa* in the suspensions was adjusted to fall within the 1~5×10^8 colony-forming units per milliliter (CFU•mL^{-1}). It is worth noting that the bacterial suspensions were prepared on the day of the experiment and used promptly to ensure the accuracy and reliability of the results.

Text S3 Removal of antibiotic resistance genes

The sewage samples were subjected to three disinfection processes: UV alone, NH2Br alone, and UV/NH2Br. After each disinfection process, the treated samples were filtered, and the DNA in the samples was enriched on 0.22 μm microporous membranes. This step allowed for the concentration and collection of the DNA fragments for further analysis and characterization. For Real-Time PCR analysis, a total of ten genes were chosen for investigation, including two sulfonamide-resistant genes (*sulI* and *sulII*), seven tetracycline resistance genes (*tetQ, tetW, tetX, tetM, tetA, tetC*, and *tetO*), and one reference gene (16S rRNA). This comprehensive selection aimed to examine the presence and abundance of these specific genes in the samples under study. Real-time PCR was a sensitive and quantitative method to analyze and quantify the target genes in the treated samples. (Yang et al., 2018). SYBR fluorescent dye method was applied. The relative abundances of target genes were calculated by the equations of Pu et al. (Eqs. (1) and (2)) (Pu et al., 2018):

$$\Delta C_t = C_t(\text{target gene}) - C_t(\text{16S rRNA}) \quad (1)$$

$$F = 2^{-\Delta Ct} \quad (2)$$

Text S4. Analytical methods.

(1) Quantification of bacterial inactivation

The log reduction (LR) was calculated to appraise the inactivation effects of UV, NH_2Br and UV/NH_2Br treatments (Eq. (3)). The LR calculated by HPC results expressed the variation of cultivable bacteria with exposure time.

$$LR = \text{Log}(N_0/N) \quad (3)$$

Where, N_0 and N represent the concentration of culturable bacteria before and after treatment, respectively ($CFU \cdot mL^{-1}$), and $Log(N_0/N)$ indicates the change in logarithm of bacterial inactivation over time.

(2) Inactivation kinetics

The inactivation rate constants of inactivation in UV alone, NH_2Br alone and UV/NH_2Br were calculated from the linear parts of the inactivation curves.

(3) ATP concentration

Adenosine triphosphate (ATP) is important for cell metabolism, so when the cell membrane function properly, only trace amounts of ATP are released outside the cell, rather than leaking in large amounts. In this study, BacTiter-Glo™ reagent (G8231, Promega, USA) was used to measure extracellular ATP concentration. After centrifuged, added the reagent directly into the supernatant of the disinfected bacterial suspensions. Then measured the fluorescence signal, which was proportional to the concentration of ATP. Thus, the changes in fluorescence intensity can qualitatively represent the changes in ATP concentration.

(4) The concentrations of extracellular DNA and proteins

When the cell membranes are damaged, intracellular substances inside the cell will leak into the extracellular environment outside the cell, such as DNA and proteins. Centrifugated samples before and after treatments at 10,000 rpm for 5 min and gained the supernatant to detect the concentrations of extracellular DNA and proteins by Micro-spectrophotometer (Nano-Drop2000, USA) in triplicate.

(5) Determination of intracellular reactive oxygen species

The intracellular Reactive Oxygen Species (ROS) level under each treatment was determined by Reactive Oxygen Species Assay Kit in the study. In the Reactive Oxygen Species Assay Kit, 2', 7'-dichlorofluorescein diacetate (DCFH-DA) was the fluorescent probe. DCFH-DA can cross the cell membrane freely and be hydrolyzed by esterase to produce 2', 7'-dichlorodihydrofluorescein (DCFH), but cannot penetrate the cell membrane. Both DCFH-DA and DCFH are non-fluorescent. ROS can oxidize DCFH to generate fluorescent 2', 7'-dichlorofluorescein (DCF). The intracellular ROS level can be known through the fluorescence intensity of DCF.

1 mL treated samples were mixed with 1 μL DCFH-DA (10 mM) and then cultured with shaking at 37 ℃ for 20 min. The mixture was washed twice and re-suspended in PB to remove excess DCFH-DA clearly. The samples were transferred to a 96-well microplate and fluorescence intensity was measured by a microplate reader (Spark 10 M, Austria).

Table S1. Principal reactions and rate constants in the UV/NH_2Br process.

No.	Reaction	Rate constant	Ref.
1	$NH_2Br + h\nu \rightarrow NH_2^{\bullet} + Br^{\bullet}$	0.50±0.04 mol Es^{-1}	[1]
2	$Br^{\bullet} + NH_2Br \rightarrow NHBr^{\bullet} + H^+ + Br^-$	$1.0\times10^9\ M^{-1}s^{-1}$	[2]
3	$Br^{\bullet} + H_2O \rightarrow BrOH^{\bullet-} + H^+$	$2.5\times10^5\ M^{-1}\ s^{-1}$	[2]
4	$Br^{\bullet} + Br^- \rightarrow Br_2^{\bullet-}$	$8.5\times10^9\ M^{-1}\ s^{-1}$	[2]
5	$BrOH^{\bullet-} \rightarrow HO^{\bullet-} + Br^-$	$6.1\times10^9\ M^{-1}\ s^{-1}$	[2]
6	$^{\bullet}NH_2 + O_2 \Leftrightarrow NH_2O_2^{\bullet} \rightarrow NO + H_2O$	$1.2\times10^8 M^{-1}\ s^{-1}$	[1]
7	$^{\bullet}NH_2 + O_2 \Leftrightarrow NH_2O_2^{\bullet} \rightarrow HNO + H_2O_2$	$1.1\times10^9 M^{-1}\ s^{-1}$	[1]
8	$4NO + 2H_2O + O_2 \rightarrow 4HNO_2$	$1.2\times10^8 M^{-1}\ s^{-1}$	[1]
9	$HO^{\bullet} + NH_2Br \rightarrow NHBr^{\bullet} + H_2O$	$1.0\times10^9\ M^{-1}\ s^{-1}$	[1]
10	$Cl^- + HO^{\bullet} \rightarrow ClOH^{\bullet-}$	$4.3\times10^9\ M^{-1}\ s^{-1}$	[3]
11	$ClOH^{\bullet-} \rightarrow HO^{\bullet} + Cl^-$	$6.1\times10^9\ s^{-1}$	[3]
12	$HO^{\bullet} + Cl^- \rightarrow OH^- + Cl^{\bullet}$	$4.7\times10^8\ M^{-1}\ s^{-1}$	[4]
13	$Cl^{\bullet} + Cl^- \rightarrow Cl_2^{\bullet-}$	$8.5\times10^9\ M^{-1}\ s^{-1}$	[5]
14	$^{\bullet}OH + {}^{\bullet}OH \rightarrow H_2O_2$	$5.5\times10^9\ M^{-1}\ s^{-1}$	[6]
15	$HCO_3^- + H_2O_2 \rightarrow HCO_4^- + H_2O$	$0.33\ M^{-1}\ s^{-1}$	[7]
16	$HO^{\bullet} + HCO_3^- \rightarrow CO_3^{\bullet-} + H_2O$	$8.5\times10^6\ M^{-1}\ s^{-1}$	[8]
17	$HCO_3^- + HO^{\bullet} \rightarrow HCO_3^{\bullet} + OH^-$	$7.0\times10^7\ M^{-1}\ s^{-1}$	[9]
18	$2NH_2Br + H^+ \leftrightarrow NHBr_2 + NH_4^+$	8×10^7~$5\times10^9\ M^{-1}$	[10]
19	$HO^{\bullet} + HPO_4^{2-} \rightarrow HPO_4^{\bullet-} + OH^-$	$1.5\times10^5\ M^{-1}\ s^{-1}$	[11]
20	$HO^{\bullet} + H_2PO_4^- \rightarrow HPO_4^{\bullet-} + H_2O$	$2.0\times10^4\ M^{-1}\ s^{-1}$	[11]

21	$Br_2^{\bullet-} + NH_2Br \rightarrow NHBr^{\bullet} + H^+ + 2Br^-$	10^2~10^4 M^{-1} s^{-1}	[12]
22	$Br_2^{\bullet-} + H_2O \rightarrow HBrOH^{\bullet} + Br^-$	1.3×10^3 M^{-1} s^{-1}	[12]
23	$HBrOH^{\bullet} \rightarrow BrOH^{\bullet} + H^+$	1.0×10^8 s^{-1}	[12]

95

Table S2. The general water quality (pH, UV_{254}, and total organic carbon (TOC)) of the water samples used in this study.

	pH	TOC/ mg L^{-1}	UV_{254}
Phosphate Buffer	7.00	0.000	0.0293
Carbon filtered water	6.52	3.729	0.0276
Surface water	6.63	3.789	0.0299

Table S3. The first order rate constants (k) of in UV alone, NH_2Br alone and UV/ NH_2Br processes.

	UV (50 μW·cm^{-2})	NH_2Br (5 mg·L^{-1})	UV/NH_2Br (5 mg·L^{-1})	UV/NH_2Br (10 mg·L^{-1})	UV/NH_2Br (20 mg·L^{-1})
k	0.17512	0.05517	0.35362	0.40245	0.44149
R^2	0.9049	0.8143	0.8969	0.9040	0.9322

Table S4 The relative abundances of target genes

	Control	UV	NH_2Br	UV/NH_2Br
tetX	0.01214	0.00805	0.00995	0.0072
tetW	0.01443	0.01101	0.01083	0.01092
tetQ	0.06472	0.04585	0.0521	0.02967
tetO	0.01654	0.01358	0.01567	0.0118
tetM	0.01346	0.01162	0.01497	0.00855
tetC	1.67E-04	1.27E-04	1.66E-04	1.13E-04
tetA	0.00741	0.01006	0.00669	0.00801
sulII	0.02115	0.03428	0.02852	0.01791
sulI	0.04147	0.02771	0.04307	0.01467

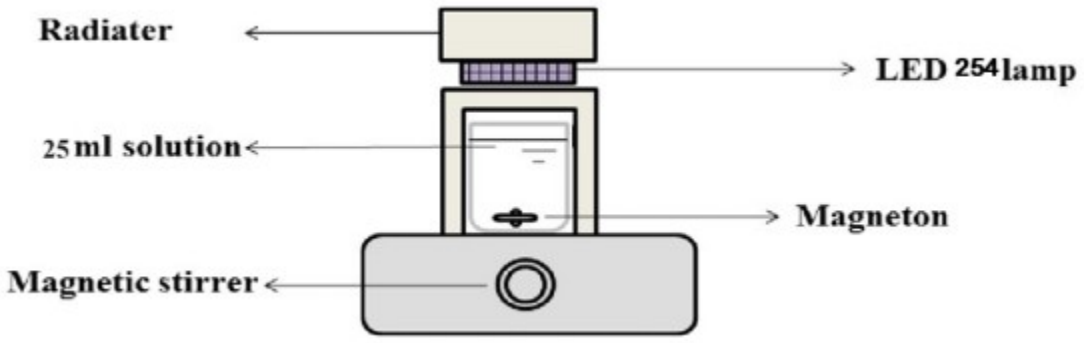

Figure S1. Schematic diagram of UV-LED (254 nm) reactor. The diameter of the round dish is 8 cm.

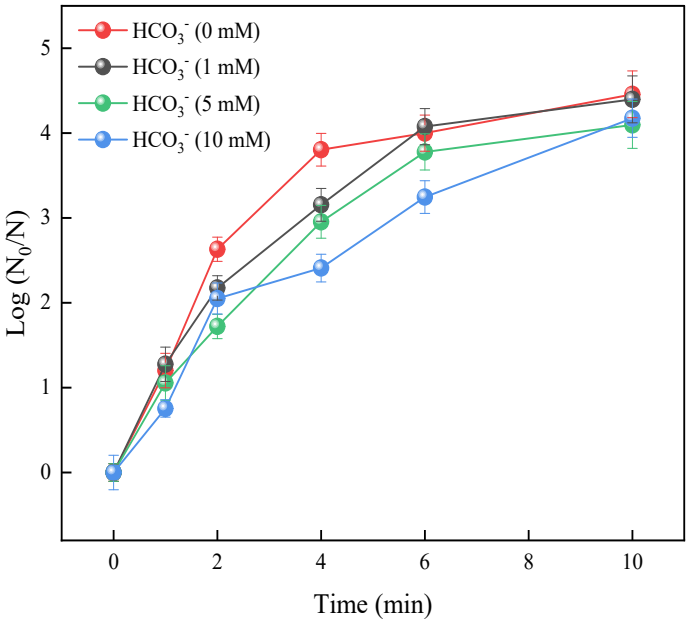

Figure S2. Inactivation of *P. aeruginosa* by UV/NH_2Br in phosphate buffer at different concentrations of HCO_3^-. Conditions: $[NH_2Br]_0$=5 mg·L^{-1}, pH=7 (buffered with 0.1 M phosphate buffer).

References

[1] L.D.W. Heasley V.L., Boerneke J.L., Boerneke M.A., Hsu H., Minnema R.A.,Moulton C.A. and Sweeney A.R., Studies on the syntheses of monobromamine NH2Br and dibromamine NHBr2 in various solvents, in, 2013.6.17.

[2] W.B. Toralf Beitz, Rolf Mitzner, Investigations of Reactions of Selected Azaarenes with Radicals in Water. 2. Chlorine and Bromine Radicals, in, 1998.1.6.

[3] J. Wang, S. Wang, Effect of inorganic anions on the performance of advanced oxidation processes for degradation of organic contaminants, Chemical Engineering Journal, 411 (2021).

[4] M. Ahmadi, F. Ghanbari, A. Alvarez, S. Silva Martinez, UV-LEDs assisted peroxymonosulfate/Fe2+ for oxidative removal of carmoisine: The effect of chloride ion, Korean Journal of Chemical Engineering, 34 (2017) 2154-2161.

[5] Z. Wu, J. Fang, Y. Xiang, C. Shang, X. Li, F. Meng, X. Yang, Roles of reactive chlorine species in trimethoprim degradation in the UV/chlorine process: Kinetics and transformation pathways, Water Res, 104 (2016) 272-282.

[6] F. Ali, J.A. Khan, N.S. Shah, M. Sayed, H.M. Khan, Carbamazepine degradation by UV and UV-assisted AOPs: Kinetics, mechanism and toxicity investigations, Process Safety and Environmental Protection, 117 (2018) 307-314.

[7] H.Y.a.D.E. Richardson, Bicarbonate Surfoxidants: Micellar Oxidations of Aryl Sulfides with Bicarbonate-Activated Hydrogen Peroxide, (2002.06.26).

[8] L. Bu, S. Zhou, S. Zhu, Y. Wu, X. Duan, Z. Shi, D.D. Dionysiou, Insight into carbamazepine degradation by UV/monochloramine: Reaction mechanism, oxidation products, and DBPs formation, Water Res, 146 (2018) 288-297.

[9] Y. Yang, J.J. Pignatello, J. Ma, W.A. Mitch, Comparison of halide impacts on the efficiency of contaminant degradation by sulfate and hydroxyl radical-based advanced oxidation processes (AOPs), Environ Sci Technol, 48 (2014) 2344-2351.

[10] M.B. Heeb, J. Criquet, S.G. Zimmermann-Steffens, U. von Gunten, Oxidative treatment of bromide-containing waters: formation of bromine and its reactions with inorganic and organic compounds--a critical review, Water Res, 48 (2014) 15-42.

[11] Y. Wu, Y. Yang, Y. Liu, L. Zhang, L. Feng, Modelling study on the effects of chloride on the degradation of bezafibrate and carbamazepine in sulfate radical-based advanced oxidation processes: Conversion of reactive radicals, Chemical Engineering Journal, 358 (2019) 1332-1341.

[12] PATTON S, LI W, COUCH K D, et al. Impact of the Ultraviolet Photolysis of Monochloramine on 1,4-Dioxane Removal: New Insights into Potable Water Reuse [J]. Environmental Science & Technology Letters, 2016, 4(1): 26-3

[13] Z. Xue, C.M. Hessler, W. Panmanee, D.J. Hassett, Y. Seo, Pseudomonas aeruginosa inactivation mechanism is affected by capsular extracellular polymeric substances reactivity with chlorine and monochloramine, Fems Microbiol Ecol, 83 (2013) 101-111.

[14] E. Bedard, M. Prevost, E. Deziel, Pseudomonas aeruginosa in premise plumbing of large buildings, Microbiologyopen, 5 (2016) 937-956.